

RV ARAON research activities within US EEZ waters in 2015

1. Overview

Araon Arctic Cruise (ARA06B) departed Nome, Alaska on July 31, 2015 and returned to Barrow on August 22, 2015. With funding provided by the Ministry of Oceans and Fisheries (MOF) and by Korea Polar Research Institute (KOPRI), the aim of the cruise was to investigate the structure and processes in the water column and subsurface (sediment) around the Bering/Chukchi/Beaufort/East Siberian Seas in rapid transition. The research effort was the conducted research cruise of the Korea-Polar Ocean in Rapid Transition (K-PORT) Program with support from the MOF and the KOPRI. Total of 54 scientists have participated from 8 countries (Korea, US, China, Japan, U.K., France, India, Spain) representing 13 different universities and research organizations. Araon data were collected on the physical, biological, chemical, and biogeochemical properties the US EEZ waters (Fig. 1.1).

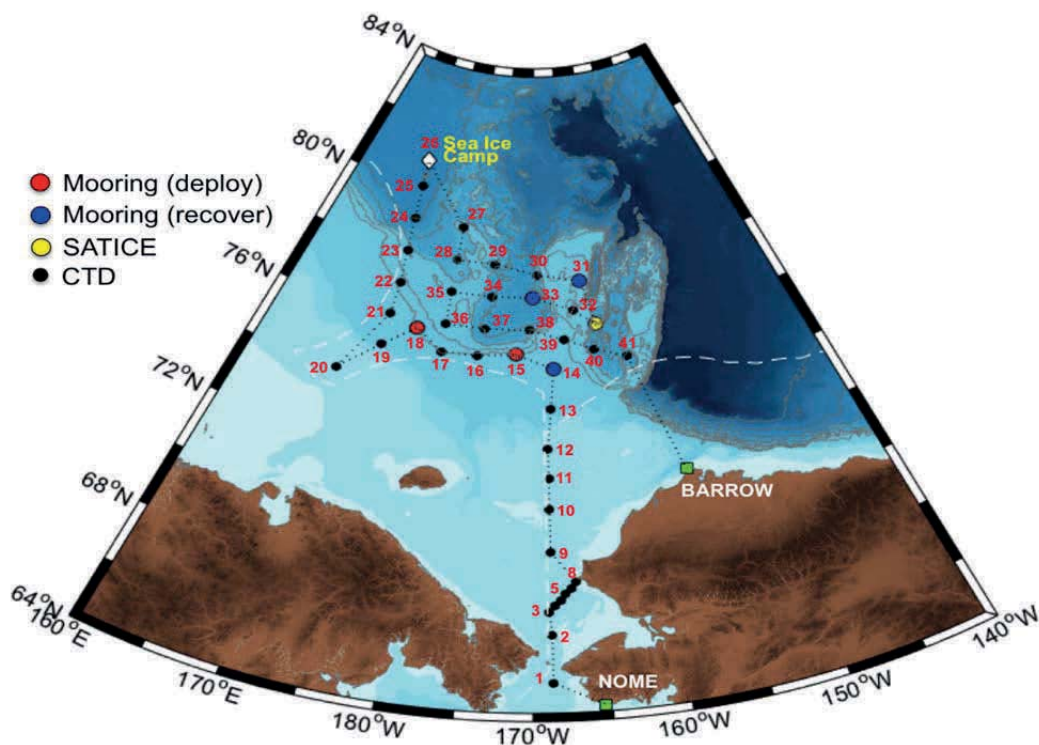


Figure 1.1. Station site (station 1-12) shown on the bathymetric chart. US EEZ boundaries are shown by black dotted line

2. Research activities

1) Physical Oceanography

An intensive oceanographic survey with 12 hydrographic stations was conducted in the Chukchi Sea within US EEZ during the period of August 1 to August 4, 2015 (Fig. 1.1). Along the transect of hydrographic stations, vertical profiles of temperature, salinity, density, dissolved oxygen, fluorescence, transmissivity and PAR, and water samples were obtained from the hydro-casts of a SBE32 carousel water sampler equipped with a SBE9plus CTD profiler, a SBE43 dissolved oxygen sensor, a transmissometer, PAR and fluorometer, and 24 position rosette with 10-liter Niskin bottles. During the CTD upcasting, water samples were collected at several depths for biochemical analyses. For the precise reading, the salinities of collected water samples were further analyzed by an Autosal salinometer (Guildline, 8400B). The measurement was performed when the temperature of water samples was stabilized to a laboratory temperature, usually within 24-48 h after the collection.

2) Nutrients and dissolved and particulate organic carbon and nitrogen in the Arctic Ocean

Seawater sampling for nutrients (PO_4 , NO_2+NO_3 , NH_4 , and SiO_2), dissolved organic carbon and nitrogen (DOC and DON) and particulate organic carbon and nitrogen (POC and PON) was carried out at 12 stations over the Chukchi Sea using a CTD/rosette sampler holding 24-10 L Niskin bottles (SeaBird Electronics, SBE 911 plus) during Korea research ice breaker R/V Araon cruise (ARA06B, August 2– 4, 2015) (Fig. 1.1)

i. Nutrients

Samples for nutrients were collected from the Niskin bottles into 50 ml conical tubes and immediately stored in a refrigerator at 2°C prior to chemical analyses. All nutrients samples were analyzed onboard within 3 days. Concentrations of nutrients were measured using standard colorimetric methods adapted for use on a 4-channel continuous Auto-Analyzer (QuAatro, Seal Analytical). The channel configurations and reagents were prepared according to the 'QuAatro Applications'. Standard curves were run with each batch of samples using freshly prepared standards that spanned the range of concentrations in the

samples. The r^2 values of all the standard curves were greater than or equal to 0.99. In addition, reference materials for nutrients in seawater (RMNS) provided by 'KANSO Technos' (Lot. No. 'BV') were used along with standards at every batch of run in order to ensure accurate and inter-comparable measurements.

ii. Dissolved organic carbon and nitrogen

For DOC and DON measurements, seawater sample was drawn from the Niskin bottle by gravity filtration through an inline pre-combusted (at 550°C for 6 hours) Whatman GF/F filter held in an acid-cleaned (0.1 M HCl) polycarbonate 47 mm filter holder (PP-47, ADVANTEC). The filter holder was attached directly to the Niskin bottle spigot. The filtrate was collected in an acid-cleaned glass bottle and then distributed into two pre-combusted 20 ml glass ampoules with a sterilized serological pipette. Each ampoule was sealed with a torch, quick-frozen, and preserved at -24°C until the analysis in our land laboratory. Analyses of DOC and DON were performed by high temperature combustion using a Shimadzu TOC-L analyzer equipped with an inline chemiluminescence nitrogen detector (Shimadzu TNM-L). Milli-Q water (blank) and consensus reference material (CRM, 42–45 μM C, deep Florida Strait water obtained from University of Miami) were measured every sixth analysis to check the accuracy of the measurements. The precision of the DOC measurements was 2–3 μM or a CV of 3–5%.

iii. Particulate organic carbon and nitrogen

For determination of POC and PON, seawater sample was drawn from the Niskin bottle into an amber polyethylene bottle. Known volumes (2 L) of seawater were filtered onto pre-combusted Whatman GF/F filters (25 mm) using a nitrogen gas purging system under gentle vacuum at < 0.1 MPa. To prevent data scattering, large zooplankton (e.g., copepods) were removed from the filter samples using tweezers after washing with filtered seawater if they were captured on the filters. These filter samples were stored at -24°C until the analysis in our land laboratory. Before POC analyses, the filter samples were freeze-dried, and then exposed to HCl fumes for 24 h in a desiccator to remove inorganic carbon from the samples. Measurements were carried out with a CHN elemental analyzer (vario MACRO cube, Elementar, Germany). Acetanilide was used as a standard. The precision of these measurements was $\pm 1.0 \mu\text{mol L}^{-1}$.

3) Air-sea CO₂ exchange and water column carbonate

i. Air-sea CO₂ flux

CO₂ flux across the sea surface is usually determined by the concentration difference between the dissolved CO₂ in the surface mixed layer and the atmospheric CO₂ overlying the surface with a parameterized gas transfer velocity k . Dissolved CO₂, so called $p\text{CO}_2$, was determined using an aqueous and gaseous phase equilibration technique with a small Weiss-type equilibrator. The air above the surface was withdrawn from the intake cup mounted at the foremast at 29 m above sea-level. The CO₂ in the air and the equilibrator headspace was analyzed with Li-cor 7000 in which 4.5 μm wavelength of photon is selectively absorbed by CO₂. The analyzing system was calibrated every 6 hours using a series of calibration gases and one zero air. $p\text{CO}_2$ in the seawater was acquired every minute in a computer and atmospheric CO₂ every 6 hours. The raw data was corrected for the effect of temperature difference between the in-situ and the equilibrator after coming back to the institute, and gas transfer velocity was determined using parameterization with wind speed which has been logged in DADIS onboard Araon.

ii. Air-sea CH₄ and N₂O flux

Methane (CH₄) and nitrous oxide (N₂O) are important greenhouse gases after CO₂ on Earth. We used a gas chromatograph (GC) to measure these gases dissolved in the ocean. The seawater was pumped into a 20-L equilibrator standing in the laboratory to collect dissolved gases which were pumped into the GC inlet, analyzed in the columns, and detected in FID and ECD to spit out electric signals. The analyzing system including the GC was calibrated with a series of calibration gases. Like the case of CO₂, the air-sea fluxes of these gases were estimated using the difference of concentrations between the atmosphere above the interface and the dissolved gases and the gas transfer velocity estimated using wind speed and parameterizations.

iii. Carbonate system of the water column

Carbonate system in the water column compose of ionic form of carbonate (CO₃²⁻), bicarbonate (HCO₃⁻), hydrogen ion (hydronium) and neutral form of carbonic acid and

dissolved CO₂. These carbonate species exist in equilibrium in seawater depending on alkalinity of the seawater. These species, however, cannot be analyzed directly using analytical instruments except CO₂ and hydronium. Thus, to determine the carbonate system in the water column, we measure total dissolved inorganic carbon (DIC) and total alkalinity (TA) by which one can derive ionic and neutral form of carbonate system. DIC and TA are defined as follows:

$$\text{DIC} = [\text{HCO}_3^-] + [\text{CO}_3^{2-}] + [\text{CO}_2] + [\text{H}_2\text{CO}_3]$$

$$\text{TA} = [\text{HCO}_3^-] + 2[\text{CO}_3^{2-}] + \Sigma[\text{anions}] - \Sigma[\text{cations}]$$

DIC and TA were analyzed in the laboratory after collecting seawater samples aboard at the hydrographic stations. To prevent the seawater samples from being altered due to biological activities in the seawater, 100 uL of HgCl₂ solution (50%) were injected upon collecting the samples from the Niskin seawater collected attached in CTD/Rosette. The sample bottles were flushed 3 times before starting collection in 250 mL bottle. Making small headspace, injecting HgCl₂ solution, and tightening the lid with black electric tape, the samples were stored in a dark place before analysis.

We also collect seawater samples for analysis of pH onboard. The procedure of collection is the same as that for DIC and TA.

To analyze dissolved CO₂ in the water column, a specially designed bottle was employed to avoid contact with ambient air onboard. The bottle composes of one stopcock and septum lid on both sides. Seawater flows through these two ends and the body of the bottle which was upright overflowing a certain time period to flush the bottle and to get rid of any bubbles inside. Upon collecting the seawater, 50 mL of CO₂ free N₂ gas was injected into the jar to equilibrate it with the water in. The equilibrated headspace air was then analyzed onboard or in the laboratory. 40 uL of HgCl₂ was injected to avoid contamination from biological activities.

4) Microbial Oceanography

During the Araon cruise in 2015, prokaryotic (i.e. Bacteria and Archaea) and viral abundances were measured at stations 4, 6 and 8 within US EEZ waters. In addition,

environmental genomic DNAs of prokaryotes and viruses were obtained and preserved as archives for future study. Sampling and analysis methods are shown in detail in the following.

Seawater sampling for microbiological study was made at 3 stations. Samples were collected from 3 depths (surface to ca. 50 m) with 10 l Niskin bottles mounted on a CTD rosette. For measurements of viral and prokaryotic abundances, seawater samples (10 ml) were fixed with 0.02 μm filtered formalin (final conc. of 2%), and were stored at -80°C .

Seawaters (4 L) for collecting genomic DNAs of prokaryotes were pre-filtered through 3.0 μm pore-sized Nuclepore filters (Whatman) and concentrated onto 0.2 μm pore-sized Nuclepore filters (Whatman). Filters were immediately transferred to cryovial tubes containing 1 ml RNAlater (Ambion) to avoid decomposition of nucleic acids, and stored at -80°C . In a land-based laboratory, extraction of nucleic acids was made as previously described by Bowman et al. (2012).

5) Photosynthetic pigments, chlorophyll-a concentrations and phytoplankton communities

The photosynthetic pigments and chlorophyll-a data were collected in the Chukchi Sea in 2015. A total of 9 stations were visited. Water samples were collected at 4-6 depths (Surface, 10m, 20m, 30m, 50m, 100m, and subsurface chlorophyll-a maximum depth) with a rosette sampler equipped with 10 L Niskin-type bottles, an in situ fluorometer, and a high-precision Sea-Bird plus CTD probe.

Subsamples from the Niskin bottles were filtered through a cascade connection of 20- μm nylon mesh, Nuclepore filter (Whatman International) with pore size of 2 μm , and a Whatman GF/F filter to determine size-fractionated chlorophyll-a concentrations. Thus, micro (>20 μm), nano (2-20 μm), and pico-sized (<2 μm) chlorophyll-a concentrations could be measured directly. Subsamples for total chlorophyll-a were filtered onto 47 mm GF/F Whatman filters. Each filter was extracted in 90% acetone for 24 hours at 4 $^{\circ}\text{C}$ in darkness, and chlorophyll-a concentrations were measured with a fluorometer (model Trilogy, Turner Designs, USA; method: Parson et al., 1984).

For photosynthetic pigments' analysis, 2 – 4 L seawater samples of surface and SCM layers were filtered onto 47 mm GF/F Whatman filters and stored at –80 °C. The filters were extracted with 3 mL 100 % acetone, ultrasonicated for 30 sec and maintained under 4 °C in dark for 15 hours. Debris was removed by filtering through 0.45 µm Teflon syringe filters. Just before injection, the extracts were diluted with distilled water to avoid the peak distortion of the first eluting pigments. Pigments were assessed by HPLC (Agilent series 1200 chromatographic system, Germany) with C8 column (Agilent XDB-C8, USA) following the method of Zapata et al. (2000).

To analysis phytoplankton community composition, water samples were obtained with a CTD/rosette unit in 20 L PVC Niskin bottles during the 'up' casts. Aliquots of 125 mL were preserved with glutaraldehyde (final concentration 1%). Sample volumes of 50 to 100 mL were filtered through Gelman GN-6 Metrical filters (0.45 µm pore size, 25 mm diameter). The filters were mounted on microscopic slides in a water-soluble embedding medium (HPMA, 2-hydroxypropyl methacrylate) on board. The HPMA slides were used for identification and estimation of cell concentration and biovolume. The HPMA-mounting technique has some advantages over the classical Utermöhl sedimentation method. Samples were also collected via phytoplankton net tows (20 µm mesh) and preserved with glutaraldehyde (final concentration 2%); these samples were used only for identification of small species in the phytoplankton assemblage. Since the results from this can be biased towards larger specimens, these data were not used for statistical analysis, but only for morphological and systematic analysis.

6) Primary production and macromolecular composition

ARAON Arctic Cruise (ARA06B) in the US EEZ was conducted from August 1 to 4, 2015. The Arctic environment is changing rapidly due to global warming and anthropogenic activities. In particular, phytoplankton as the primary producer is sensitive to changes in the marine conditions, which can affect higher trophic levels. Therefore, studies on the primary productivity and biochemical composition of phytoplankton are needed to understand present status and predict the future of marine ecosystems in the Arctic.

First, water samples were obtained from six light depths (100, 50, 30, 12, 5, and 1 %)

using a CTD rosette sampler. To estimate carbon and nitrogen uptake rates of phytoplankton, stable isotope reagents (^{13}C , $^{15}\text{NO}_3$, $^{15}\text{NH}_4$) were added to each bottle and then incubated for 4-5 hours on the deck under the natural light (Figure 3.6.1). After incubation, samples were filtered through GF/F (Whatman, 0.7 μm pore, $\varnothing = 25$ mm) filter paper and stored at -80 $^\circ\text{C}$ until analysis. Both carbon and nitrogen isotope abundances were determined by a IRMS (Isotope-ratio mass spectrometer) in the physical research laboratory Ahmedabad, India after the carbonate removal. For background data, water samples were collected alkalinities and major nutrient concentrations (nitrate, nitrite, and ammonium).

Second, water samples for macromolecular composition of phytoplankton obtained from 3 light depths (100, 30, and 1%). Each seawater sample went through a 47 mm GF/F filter (Whatman, 0.7 μm pore) and was then immediately stored at -80 $^\circ\text{C}$ prior to biochemical analysis. The content of carbohydrates was determined by phenol-sulfuric method from Dubois et al. (1956) and particulate protein content was determined by the Lowry method (1951). For lipid extraction and assay from 1:2 (v/v) chloroform-methanol mixture and tripalmitin solutions were used (Bligh and Dyer, 1959; Marsh and Weinstein, 1966). The three particulate organic extracts from a blank GF/F filter were used as controls.

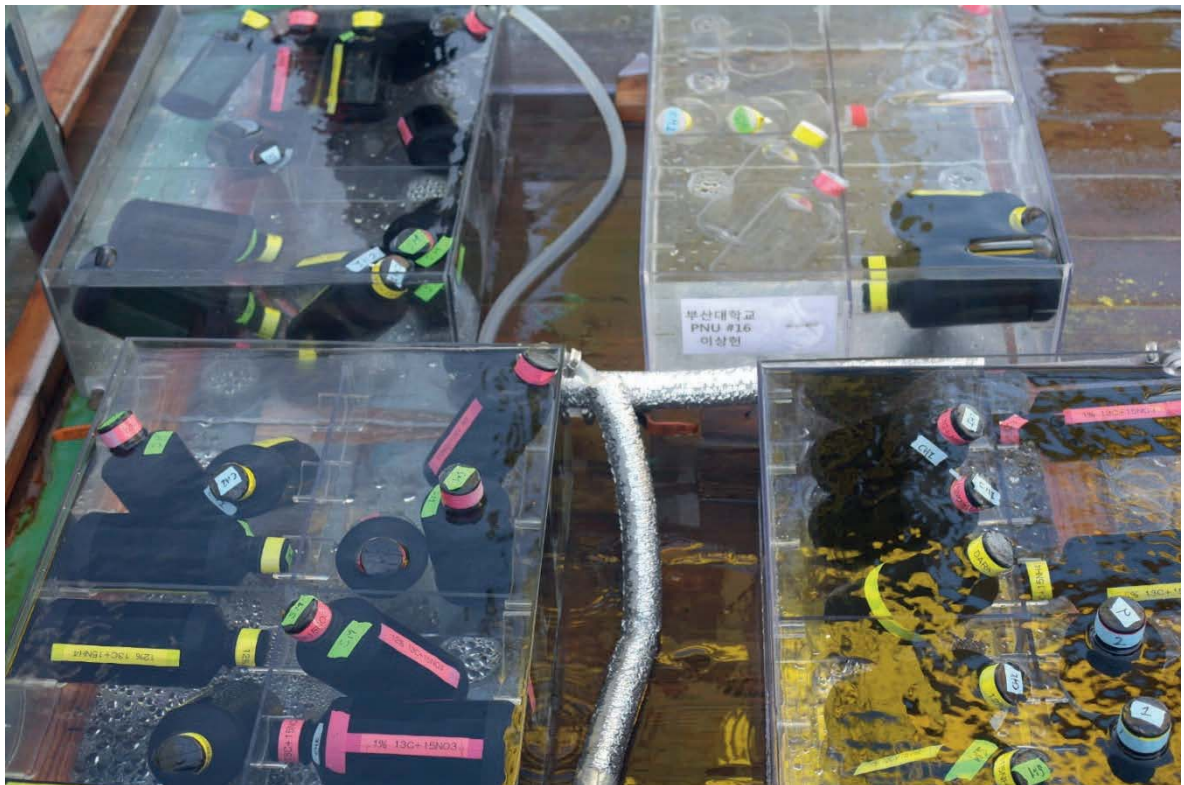


Fig. 2.6.1. *In situ* incubation on the deck for 4-5 hours.

7) Nitrogen stable isotope ratio of zooplankton

Nitrogen isotope analysis for background nitrogen in Arctic waters was performed using zooplankton, *Calanus Hyperboreus*(Figure 2.7.1). The zooplankton samples were collected by using 500 μm net, and stored in deep freezer(-80 ° C). The samples were transferred to the laboratory and lyophilized. The lyophilized zooplankton samples were homogenized using a mortar bowl to analyze amino acids and bulk nitrogen isotopes.

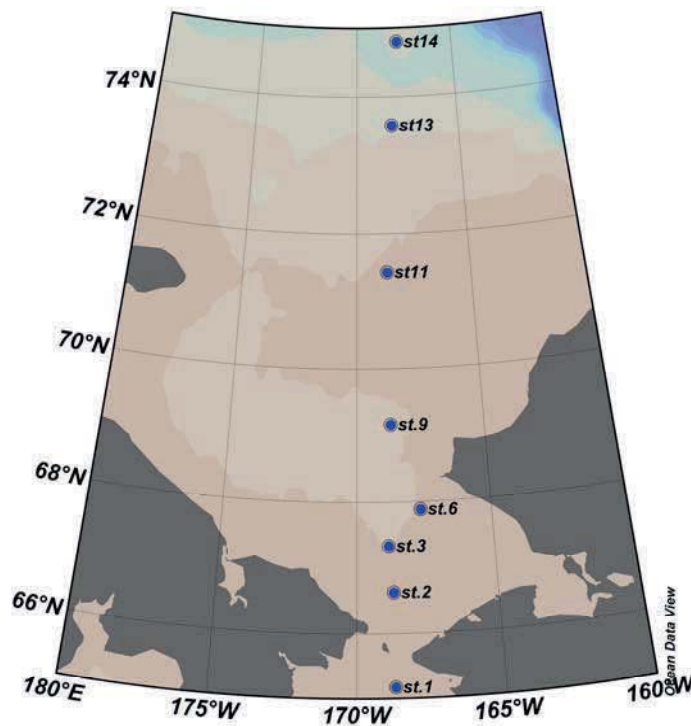


Fig. 2.7.1. Sampling stations.

Bulk nitrogen stable isotope ratio of zooplankton was analyzed using a stable isotope mass spectrometer (EA-IRMS) interlocked with an elemental analyzer. As a oxidation column of EA, quartz tube filled with Chromium oxide and Cobalt oxide was used at 1020°C, and as a reduction column, quartz tube filled with Copper was used at 650°C. During the analyze of each samples, we determined the degree of accuracy through performing repetitive analyze

of N-1(0.4‰, IAEA).

The nitrogen stable isotope ratio of zooplankton amino acid was analyzed using GC-IRMS, which is isotope ratio mass spectrometer interlocked with gas chromatography, after hydrolysis, lipid removal, derivatization. As a oxidation column of GC-IRMS, quartz tube filled with copper oxide, nickel oxide and platinum wire was used at 950°C, and as a reduction column, ceramic tube filled with copper and rhodium wire was used at 650°C. GC column, which is for separating each amino acid compounds, was HP-ultra-2(Agilent, USA). The flow rate was 1.0ml/min during analyze. The standard deviation of reference gas stability in the IRMS was less than 0.1‰, and we confirmed precision through analyzing standard after analyzing each three samples.

8) Protozoa abundance and grazing rates on phytoplankton

To determine the abundance of heterotrophic protists, a CTD-Niskin rosette sampler was used to take water samples from the following 4-6 depths. For ciliates, 500 ml water from the vertical profiles was preserved with 1% acid Lugol's iodine solution these samples were then stored in darkness. For heterotrophic nanoflagellates and heterotrophic dinoflagellates smaller than 20 µm, 500 ml of water was preserved with glutaraldehyde (0.5% final concentration) and stored at 4°C. Grazing rates of heterotrophic protists on phytoplankton were determined by the dilution method (Landry and Hassett 1982). Water for grazing experiments was collected from 2 depths (surface, SCM) of each station, and gently filtered through a 200-µm mesh. At each station, 30L seawater were collected in a Niskin bottle and transferred to a polycarbonate carboy. Part of this water was filtered through the 0.22-µm filtration system. Dilution series were set up in ten 1.3-l PC bottles. Ten bottles were used to establish a nutrient-enriched dilution series consisting of replicate bottles with 20 and 100% natural seawater. The bottles were incubated on deck for 24-48h at ambient sea surface temperatures and screened to the ambient light level with neutral density screening. Subsamples were collected from replicate bottles at 0 and 24-48h to determine chlorophyll-a concentrations.

9) Mesozooplankton abundance and composition

To estimate the abundance of zooplankton and its compositions, net samples were collected with a Bongo net (60 cm diameter, 330 and 500 μm mesh) at 9 selected stations. The net was towed vertically within the upper 200 m of the water column for about 10 – 15 min. The filtering of seawater for each sample was indicated by revolution counts of a flow meter attached to the net. The half of samples from 330 μm net was immediately fixed and preserved with 10% neutralized formaldehyde for quantitative analyses. Subsampling will be carried out using a Folsom plankton splitter, and abundance will be expressed in terms of individual numbers per cubic meter using volume filtered by net, obtained from the revolution counts of a flow meter attached to the net. Subsamples from 500 μm net were transferred to 20-ml vials with natural seawater, which were frozen at $-80\text{ }^{\circ}\text{C}$ for the post analysis.

10) Phytoplankton physiology (photochemistry)

To investigate the impact of physico-chemical conditions on photosynthesis in the study area, we measured photosynthetic characteristics of phytoplankton at total 12 stations (including six DBO stations) using a Fluorescence Induction and Relaxation (FIRe) system (Fig. 2.10.1). Continuous measurements also conducted underway (using pumped on seawater around 7 m depth beneath the ship) during the Araon transit. Active fluorometry is a non-destructive and rapid method, and it has been used to monitor variations in the photochemistry (Kolber and Falkowski, 1993; Falkowski and Kolber, 1995). These measurements provide an express diagnostics of the effects of environmental factors on photosynthetic processes such as nutrient limitation. After collection from Niskin bottles at 5 - 6 depths within 100 m, samples were kept under in situ temperature in light bottles. These samples were measured after 30 minutes' low light adaptation. Photosystem II (PSII) parameters such as the minimal fluorescence yield (F_0 ; when all reaction centers are open), the maximal fluorescence yield (F_m ; all reaction centers are closed), the quantum efficiency of PSII (F_v/F_m), the functional (or effective) absorption cross-section of PSII (σ_{PSII}) were measured as describe in Kolber et al. (1998). Quantum efficiency of photochemistry in PSII (F_v/F_m) was calculated as a ratio of variable fluorescence ($F_v = F_m - F_0$) to the maximum one

(Fm). The fluorescence measurements were corrected for the blank signal recorded from filtered seawater (by 0.2 μm syringe filter set. When the ship was, underway pumped on the seawater near surface and the fluorescence was measured continuously on real time. Consequently, we also deployed another in situ profiling type of FIRE at 3 stations for measuring quantum yields according to light levels (i.e., P-E measurement).



Fig. 2.10.1. A custom-built Fluorescence Induction and Relaxation (FIRE) system onboard Araon.

11) Ocean Optical Observation

In this cruise, we tried to obtain bio-optical relationships to improve ocean color data quality by observing absorptions from phytoplankton, suspended sediment (SS), inherent optical properties (IOPs) of water (e.g. absorptions by colored dissolved organic matters (CDOM)) and apparent optical properties (AOPs) of water (e.g. downwelling irradiances (E_d) and upwelling radiance (L_u)). Our major goal in this study was to collect bio-optical data in conjunction with measurements of CDOM, phytoplankton and SS absorption in support of NASA's efforts to develop robust empirical and semi-analytic algorithms for ocean color products in high latitude regions. This effort is a part of longer strategic objective of

understanding the impacts of changing climate on biological oceanographic processes in the Arctic Ocean using ocean color satellite data.

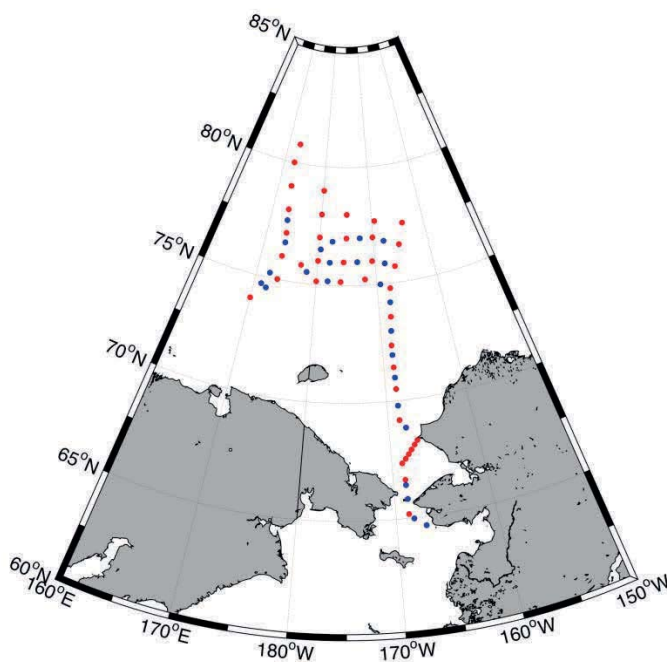


Fig. 2.11.1. A station map for ocean optical observation (red dot : station, blue dot : underway water sampling point).

We sampled 117 waters at 39 stations (with 3 depths of surface, subsurface chlorophyll maximum, and bottom within euphotic depth) and 25 intermediate sites between stations in underway route (Fig. 2.11.1). To measure inherent optical properties (IOPs) of water, seawater volumes of 500 - 2,000 ml were filtered on 25 mm glass-fiber filters. Optical densities of total particulate matters were measured directly on the wet filters by methods of Truper and Yentch (1967) with a double-beam recording spectrophotometer (Cary100, Agilent Technologies) in a spectral range 250 - 800 nm (spectrum resolution of 1 nm). The filter was placed in front of diffusing windows adjacent to an end-on photomultiplier of large surface area. For a reference blank and baseline variations, an unused wetted filter was used, and the instrument was taken as were automatically corrected. After the measurement of optical density of total pigments, the spectral absorption by non-algal material was measured separately with the method of Kishino et al. (1985).



Fig. 2.11.2. Deploy of hyper-spectroradiometer (HPRO II and TriOS).

For the measuring apparent optical properties (AOPs) of water, we deployed hyper-spectroradiometer (HPRO II and TriOS, Fig. 2.11.2) with a spectral range of 350 - 800 nm (HPRO II), 280 - 950 nm (TriOS) of downwelling irradiance (E_d) and upwelling radiance (L_u). For the reference as ambient irradiance variation, downwelling irradiance (E_s) was measured on deck in a place without shade. The integrated instruments deployed through the A-frame at the stern of the vessel. The deploying speed was 10 m/min. This data will be able to be used for calibrations and validations of currently operating ocean color remote sensing data.

12) Atmospheric Observations

Atmospheric observations on IBRV Araon include the basic surface meteorological parameters (e.g., air temperature, humidity, pressure and wind) and aerosols. All the observations were almost continuous during the cruise, so we obtained various time series along the cruise track. However, CO_2 concentrations were not observed because the eddy-covariance system was not loaded on the ship.

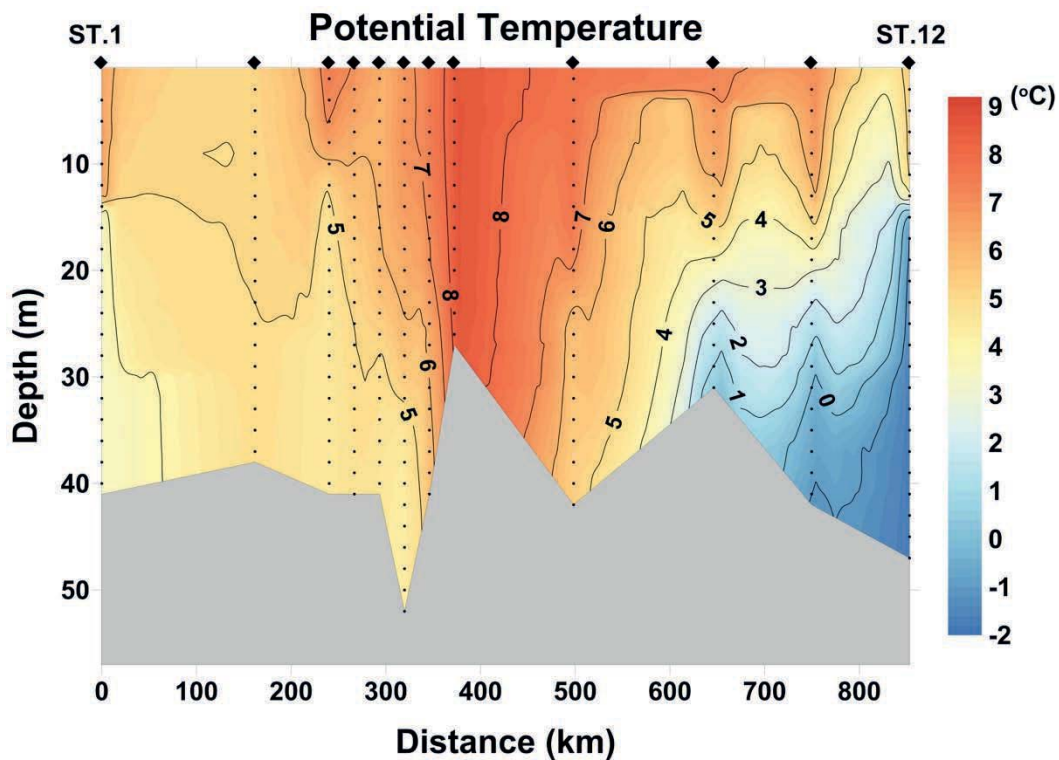
Meteorological observations on the radarmast include air temperature and relative humidity (HMP45D, Vaisala, Finland), air pressure (PTB100, Vaisala), and horizontal winds (2D sonic anemometer). The data logger (CR3000, Campbell Scientific, Inc., USA) scans each sensor every 10 seconds and saves the average of scans every 10 minute.

3. Scientific achievements

1) Physical Oceanography

i. Vertical Structures

Vertical structures of potential temperature and salinity at the transection from St. 1 to St. 12 are shown in Fig. 3.1.1 (other parameters are plotted in Fig. 3.1.2). The Pacific Water around the Bering Strait (St. 1) is specified with 3.4-6.5 °C and 32.5-32.7 psu. Salinity is vertically homogeneous but temperature difference between bottom and surface is nearly 3 °C. At St. 2, the water is vertically homogeneous representing ~5.0 °C and ~32.1 psu. From St. 3 to St. 7, water temperature ranges from 4.4 to 7.5 °C and salinity ranges from 31.8 to 32.4 psu. The water mass at St. 8 is specified with 8.5 °C and 30.3 psu representing the Alaskan Coastal Water. At St. 12, the water is relatively stratified and temperature-salinity properties range from 1.7 to 5.3 °C and from 29.6 to 32.7 psu, respectively. Surface layer is occupied by relatively warm and fresh water but lower layer is occupied by cold water.



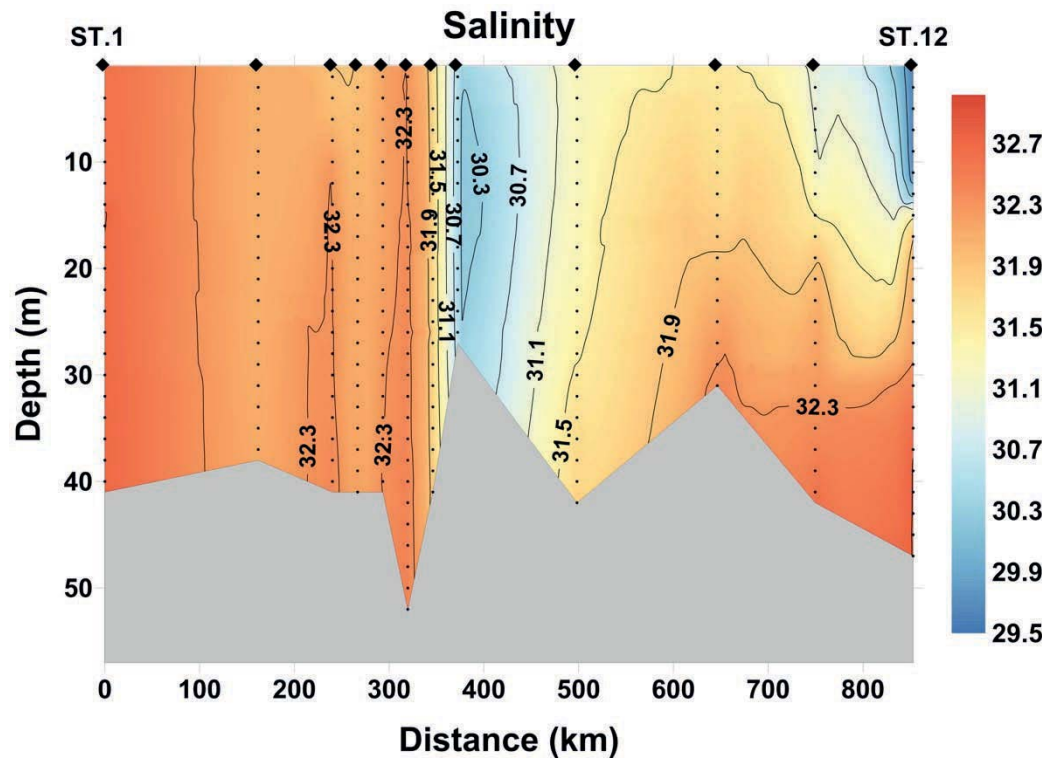
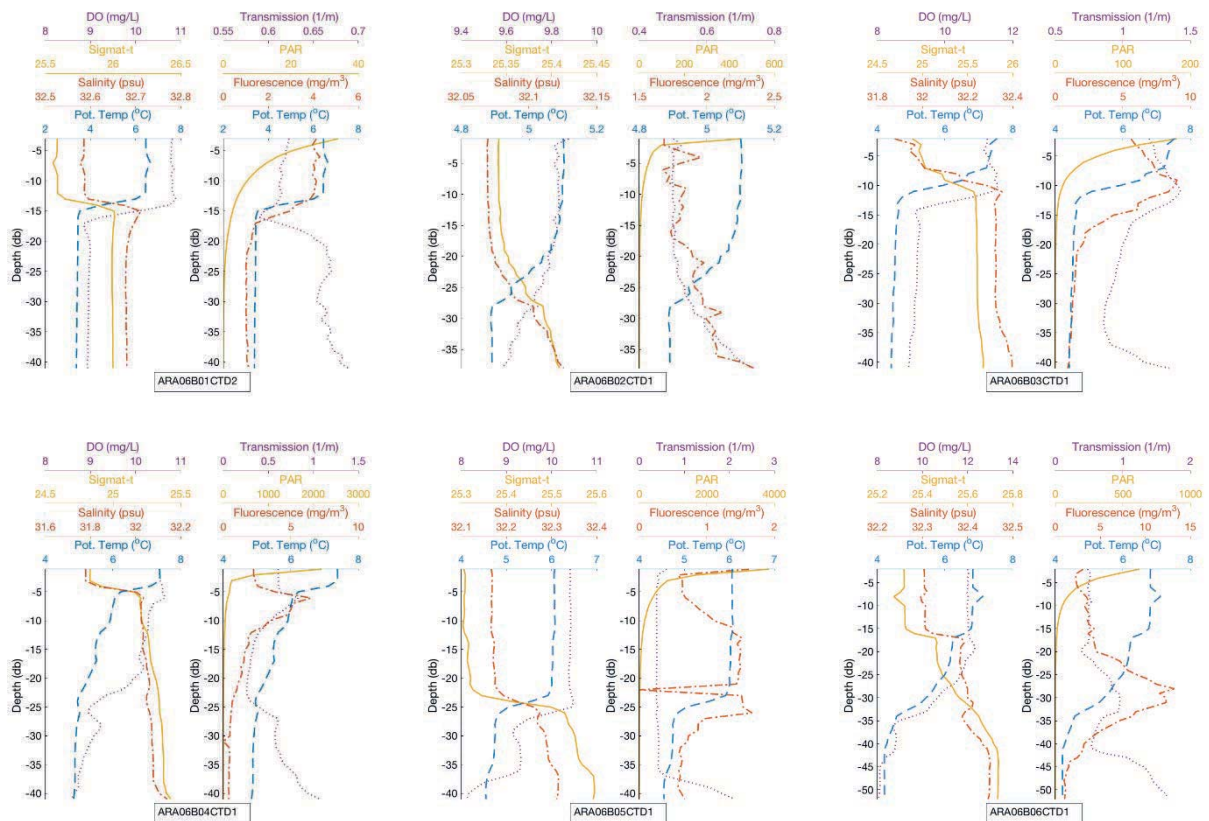


Fig. 3.1.1. Vertical structures of potential temperature (upper) and salinity (lower) at the transection from St.1 to St.12.



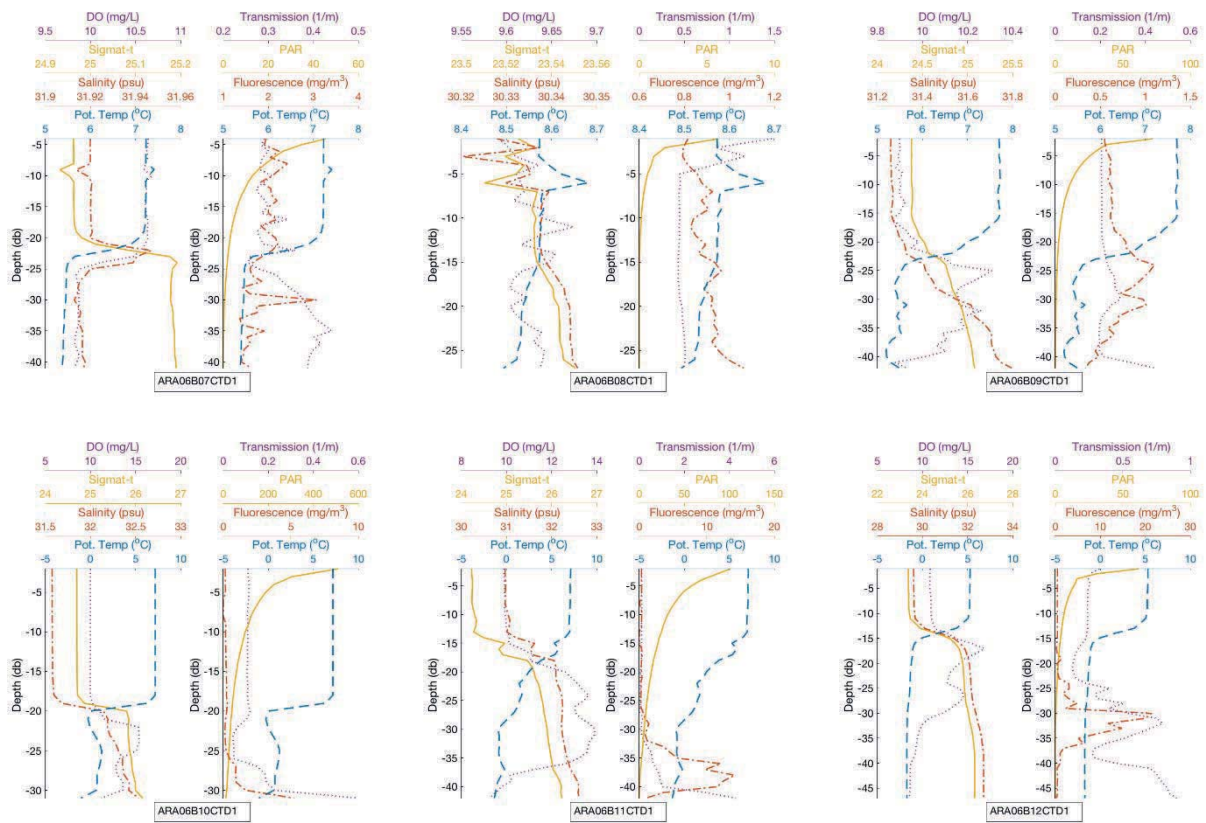


Fig. 3.1.2. Vertical structures of oceanographic parameters (potential temperature, salinity, density, dissolved oxygen, fluorescence, PAR, and transmission) from St.1 to St.12.

ii. T-S Diagram

During the expedition, 12 CTD stations were selected within US EEZ. Potential temperature () – salinity (S) diagram shows that the Chukchi Sea is occupied by several water masses: summer Bering Sea Water (BSW) coming from the Bering Strait, Alaskan coastal water (ACW) along the Alaska coastline, and cold lower layer water (Fig. 2.3)

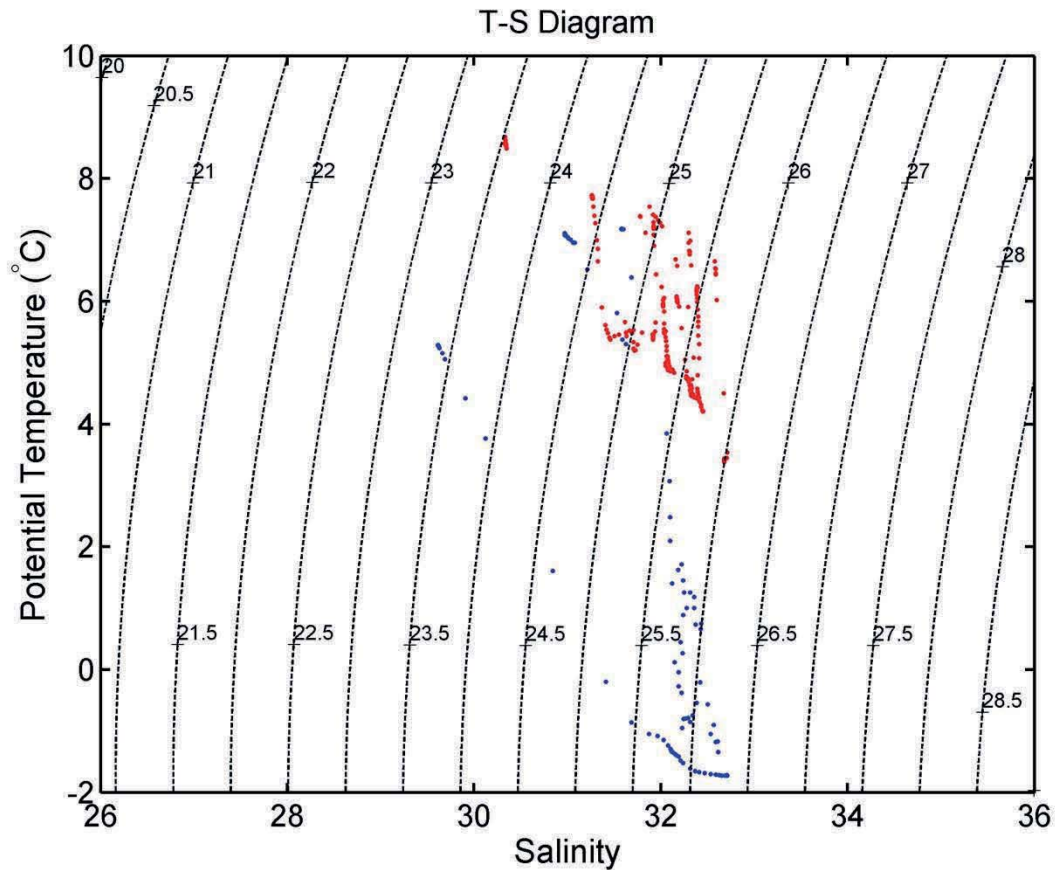


Fig. 3.1.3. Potential temperature (θ)-salinity (S) diagram using CTD data observed from hydrographic stations. Red dots are for St. 1 to St. 9 and blue dots are for St. 10 to St. 12.

2) Nutrients and dissolved and particulate organic carbon and nitrogen in the Arctic Ocean

There was an east–west gradient in water-mass properties across stations 3–8, with the highest nutrient concentrations, highest salinities, lowest temperatures generally occurring in the Anadyr Water in the west; and the lowest nutrient values, and lowest salinities and highest temperature tending to occur in Alaska Coastal Water in the east (Fig. 3.2.1). PO_4 concentration varied from 0.25-0.75 $\mu\text{mol/L}$ in the east side where the influence of Alaska Coastal Water is strong, whereas NO_2+NO_3 concentration was below detection limit, suggesting that primary production in the Arctic Ocean is limited by nitrogen. In contrast, nutrients concentration in the west, where the influence of Anadyr Water is strong, was high.

Especially, NH_4 concentration varied from 0.5~5.5 $\mu\text{mol/L}$, which is derived from the decomposition of particulate organic matter, suggesting active decomposition of particulate organic matter by bacteria in the continental shelf.

For dissolved organic matters, the highest DOC concentration was observed in the eastern side where the influence of Alaska Coastal Water was strong, suggesting that DOC was mainly derived from terrestrial sources. DON showed somewhat different distribution to that of DOC. The distributions of POC and PON were quite similar to that of chlorophyll a concentration. Moreover, the lowest concentrations of POC and PON were found in the eastern side, showing that Alaska Coastal Water is not a significant source of POC and PON, and that POC and PON were derived from marine biological activities.

Fig. 3.2.1. Salinity (a), temperature (b), PO_4 (c), NO_2+NO_3 (d), NH_4 (e), SiO_2 (f), DOC (g), DON (h), POC (i) and PON (j) concentrations in a section taken from stations 3–8 during the ARA06B cruise.

3) Air-sea CO₂ exchange and water column carbonate system

- i. Carbonate system and its control factors in the Chukchi Sea in perspective of the changing arctic environment

The Arctic Ocean lies in the center of the current climate change as the summer sea-ice extent shrinks dramatically in recent years. Several modeling studies predict complete disappearance of the sea-ice extent in summer this century. One of the concerns resulting from this rapid change in the Arctic climate is the impact on the marine ecosystem in which carbon is the backbone of the energy flow initiated by solar energy. In addition, the shift of the ice-covered to the complete open ocean may lead to the change in the CO₂ flux across the sea-surface due to the imbalance in $p\text{CO}_2$ between, which is ultimately driven by the primary production in the surface mixed layer and by the Arctic circulation. To investigate the change in the air-sea CO₂ flux and the carbonate system interior of the water column, we have visited for 5 years the Chukchi Sea every summer season since 2010 and the Beaufort Sea in 2013 and 2014 onboard the Korean ice breaking R/V Araon. The areas surveyed were always undersaturated with respect to the atmospheric CO₂ despite large variability of the degree of saturation. We explored the spatial and temporal characteristics of the carbonate system in conjunction with the extent to which physical and biological properties would influence. To identify the driving forces in changing carbonate system interior of the water column, we focused on the impact of sea-ice melting, freshwater input from the continent, enhanced biological uptake driven by primary production, and chemical processes, which allow us to delve carbon flow in these particular area. In the presentation we will discuss the results from the 5-year observations in the picture of the rapid change in the Arctic environment.

- ii. Spatial distribution of dissolved CH₄ and N₂O in the Western Arctic Ocean

Methane and nitrous oxide are the important greenhouse gases next to carbon dioxide in the atmosphere. To investigate the impact these gases on the rapid change in the Arctic climate, we surveyed these gases together with CO₂ in the Western Arctic Ocean including the Chukchi Sea, the Beaufort Sea, and the East Siberian Sea. The dissolved CH₄ were in general super-saturated with respect to the atmospheric CH₄ in the survey area while the

dissolved N_2O were not. The status of CH_4 supersaturation has been reported in the literature and in particular some of them suspected to link it to melting gas hydrate under the sediment floor due to the increase of the seawater temperature in the coastal region. It is already known that the Arctic continent release methane in the permafrost and its emission rate are accelerated in recent years due likely to the rapid temperature increase. Continual observation of these gases in the Arctic Ocean in the future will tell us the connection between the Arctic climate change and the emissions of greenhouse gases from the Arctic Ocean.

4) Microbial Oceanography

ARA06B Microbial analysis is currently underway at the laboratory in KOPRI.

5) Photosynthetic pigments, chlorophyll-a concentrations and phytoplankton communities

The photosynthetic pigments and chlorophyll-a concentrations were determined in the US EEZ waters during August 2015. A total of 9 stations were visited and water samples were collected at 4-6 depths at each station including subsurface chlorophyll-a maximum layer.

The chlorophyll-a concentration varied from 0.21 to 10.56 $\mu\text{g/L}$ with an average of 2.10 $\mu\text{g/L}$ in this region. The depth-averaged chlorophyll-a concentration was the highest at station 6 and the lowest at station 10 (Fig. 3.5.1). The micro- ($>20\mu\text{m}$) and pico- ($<2\mu\text{m}$) size chlorophyll-a concentrations made the highest and lowest contribution to total chlorophyll-a content, respectively 40.8% and 20.7% on average, indicating the large contribution of micro- and nano-size phytoplankton to primary production in this region. The subsurface chlorophyll-a maximum layer became developed between 10 to 50m depth.

The detected photosynthetic pigments of phytoplankton were chlorophyll-a, -b, -c2, -c3, fucoxanthin, alloxanthin, 19'-butanoyloxyfucoxanthin, prasinoxanthin, violaxanthin, 19'-hexanoyloxyfucoxanthin, diadinoxanthin, diatoxanthin, zeaxanthin, $\beta\beta$ -carotene, and the degradation products of chlorophyll. The major pigment of diatoms, fucoxanthin showed the

high concentration in the study area and accounted for more than 60% of total photosynthetic pigment concentration except chlorophyll-a, indicating that diatoms were the dominant group in phytoplankton biomass during the study period.

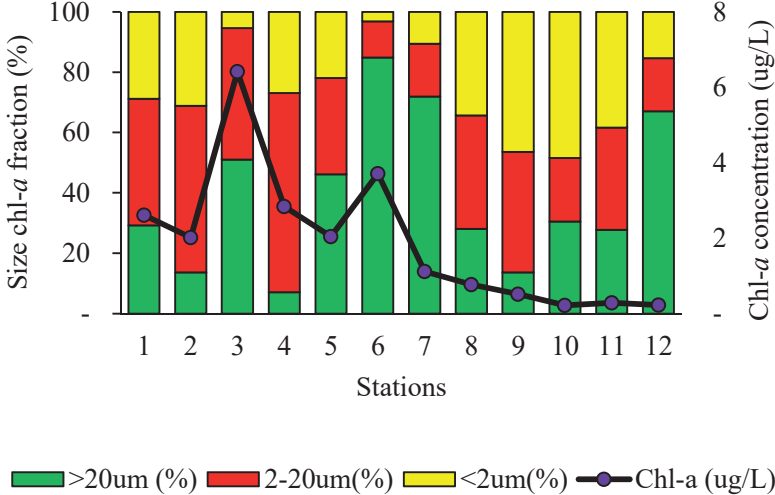


Fig. 3.5.1. The surface chlorophyll-a concentrations (μgL^{-1}) and size-fractionated chlorophyll-a fractions (%) in August 2015.

Based on the HPMA slide method and SEM analysis, the samples were made for identifying species compositions of phytoplankton later at the laboratory in KOPRI (Fig. 3.5.2)



Fig. 3.5.2 HPMA Slides for Quantity analysis of phytoplankton communities.

6) Primary production and macromolecular composition

i. Primary production and new production

The samples for primary production and new production are analyzing at the physical research laboratory, Ahmedabad, India.

ii. Phytoplankton macromolecular composition

Phytoplankton consist of important biochemical components such as proteins, carbohydrates, and lipids. The proteins play a role in biological processes such as enzymatic catalysis and growth, and transfer carbon to herbivore biomass with higher efficiency than other biomolecular classes (Stryer,1988; Lindqvist and Lignell,1997). The lipids and carbohydrates act as an energy storage and are essential components of all membranes (Handa,1969; Parrish,1987). These biochemical components are known to be sensitive to environmental factors such as water temperature, salinity, nutrient concentration, and light conditions. Therefore, it is possible to obtain important information on the physiological state of phytoplankton and understand the current environmental condition through the study of macromolecular composition of phytoplankton. Thus, it is necessary to study the macromolecular composition of phytoplankton to understand how the current environmental changes affect the arctic marine ecosystem.

The macromolecular compositions of phytoplankton were different at the 100%, 30%, and 1% light depths (Fig. 3.6.1; 3.6.2). The percentage of carbohydrates in the EEZ ranged from 18% to 61%. Protein ranged from 16% to 41% and lipid ranged from 19% to 54%. Carbohydrates, proteins, and lipids in the euphotic zone increased with increasing latitude (Fig. 3.6.3; 3.6.4; 3.6.5).

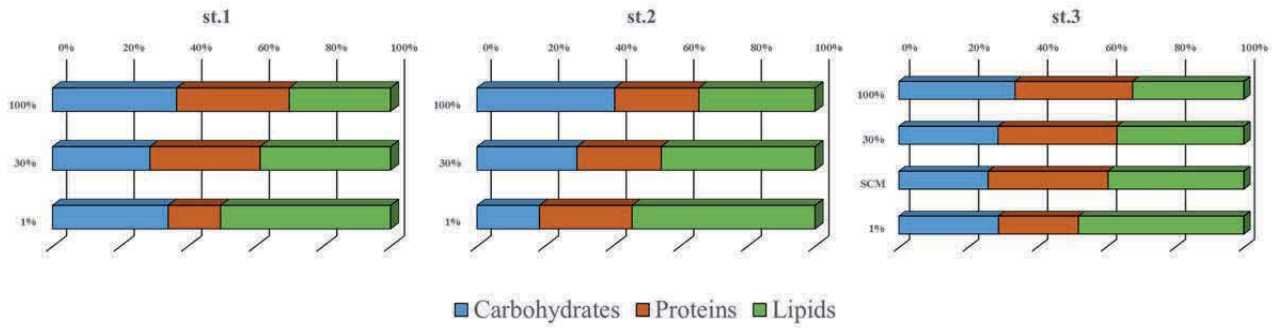


Fig. 3.6.1. Biochemical compositions of phytoplankton at st.1, 2, 3.

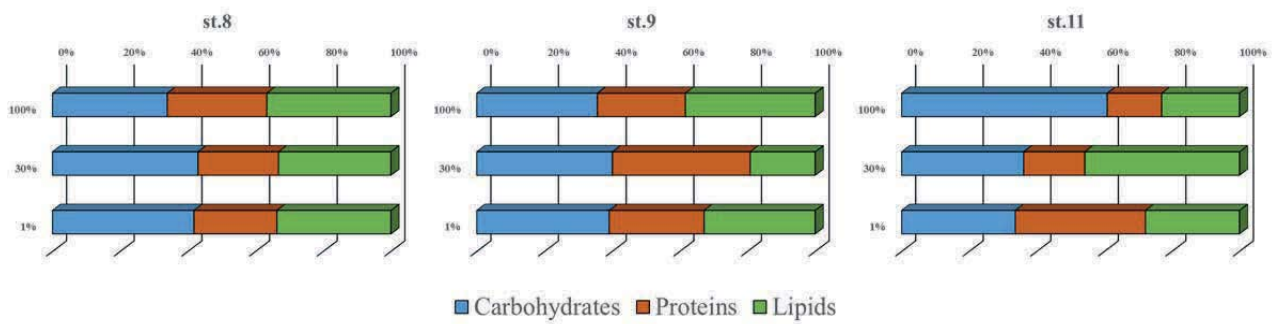


Fig. 3.6.2. Biochemical compositions of phytoplankton at st.8, 9, 11.

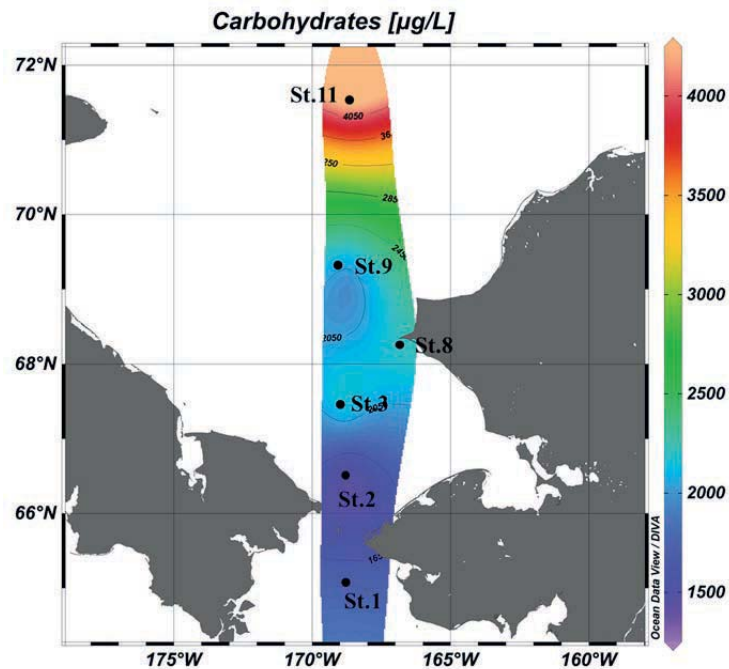


Fig. 3.6.3. Concentrations of carbohydrates in phytoplankton integrated in the euphotic zone.

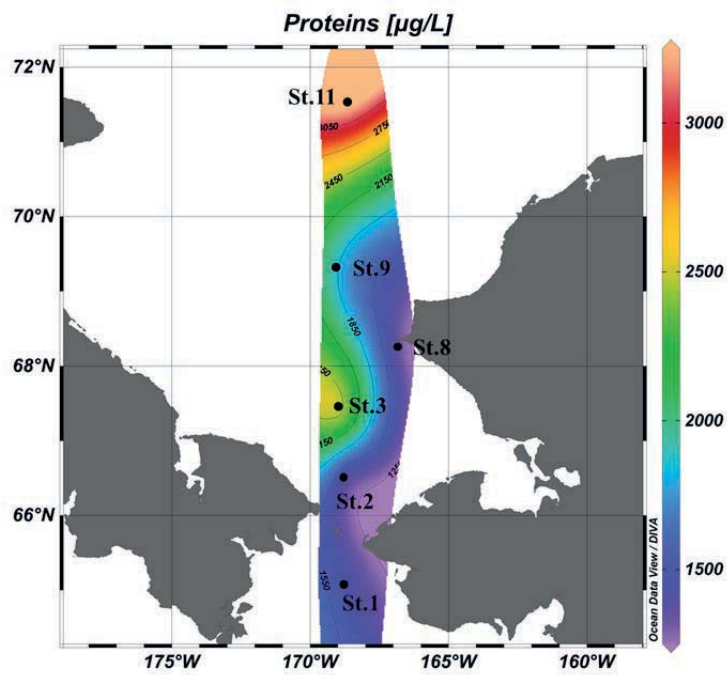


Fig. 3.6.4. Concentrations of Proteins in phytoplankton integrated in the euphotic zone.

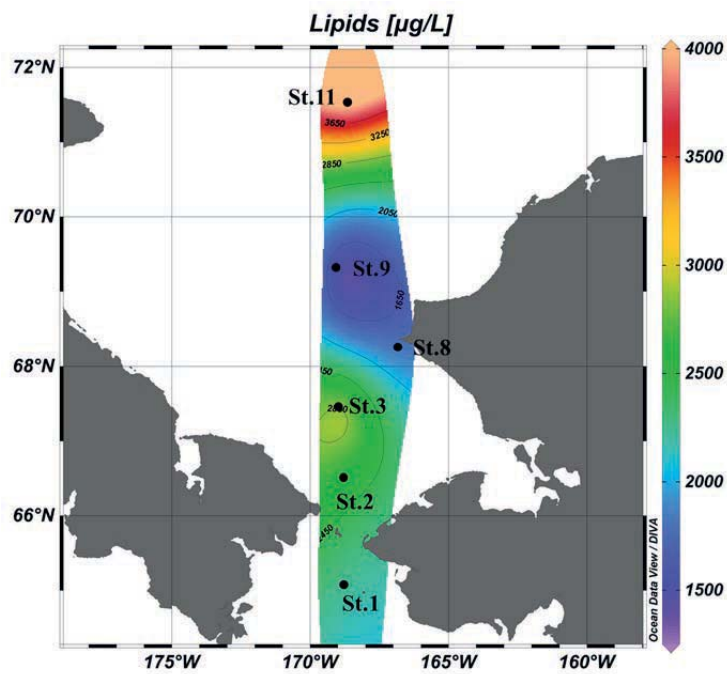


Fig. 3.6.5. Concentrations of Lipids in phytoplankton integrated in the euphotic zone.

7) Nitrogen stable isotope ratio of zooplankton

The zooplanktons' bulk and amino acid nitrogen stable isotope ratio are shown on figure 3.7.1. The phenylalanine nitrogen stable isotope ratios of zooplankton are appeared lighter than bulk nitrogen stable isotope ratios of zooplankton. This result is interpreted because the bulk nitrogen stable isotope ratios include information on the trophic position of zooplankton. The phenylalanine nitrogen stable isotope ratios of zooplankton, which reflect information on background nitrogen, are similar with the nitrogen stable isotope ratio of nitrate in seawater.

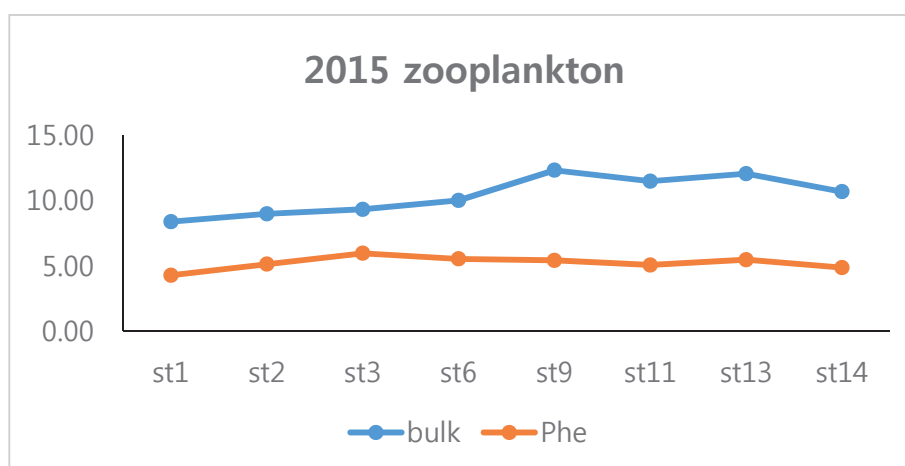


Fig. 3.7.1 Bulk and amino acid nitrogen stable isotope ratios of zooplankton.

For calculating trophic position of marine organism using amino acid nitrogen stable isotope ratio, nitrogen stable isotope ratios of glutamic acid, which is one of the trophic amino acids, and nitrogen stable isotope ratios of phenylalanine, which is one of the source amino acids, are applied in the formula below.

$$TP_{AAs} = [(\delta^{15}N_{Glu} - \delta^{15}N_{Phe} - 3.4) / 7.6] + 1 \text{ (Chikaraishi et al., 2010)}$$

In this ocean area, zooplanktons are identified omnivores because average of trophic position is 2.82 ± 0.22 (Figure 3.7.2).

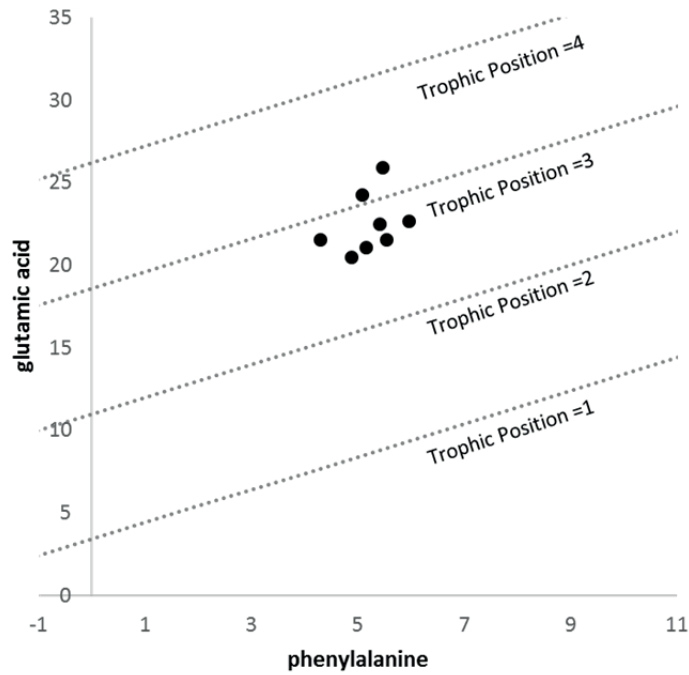


Fig. 3.7.2 Zooplanktons' trophic position calculated by utilizing glutamic acid and phenylalanine nitrogen stable isotope ratio

8) Protozoa abundance and grazing rates on phytoplankton

Heterotrophic protozoa ingest a broad size spectrum of prey, from bacteria to phytoplankton, and are themselves important prey items for mesozooplankton. Many researchers suggest that heterotrophic protist contribute to the trophic linkage between phytoplankton and mesozooplankton and are important in the pelagic food webs of many oceanic waters. The importance of heterotrophic protist in pelagic ecosystems has become increasingly evident in the past two decades, and trophic interaction between heterotrophic protists and phytoplankton has been reported in various marine. However, there is no information on the relative importance of heterotrophic protist in the pelagic ecosystem of the Western Arctic Sea. The Arctic Ocean is currently experiencing rapid environmental change due to natural and anthropogenic factor that includes warming, sea ice loss and other physical change as well as biology and ecosystem structure change. During this cruise, we investigated the meso-scale variations and structure of heterotrophic protozoan abundance and grazing rates on phytoplankton in the northern Bering Sea. In this study area, abundance of heterotrophic protozoa varied from 300 to 25,000 cells L⁻¹, and ciliates

and heterotrophic dinoflagellate were dominant in heterotrophic protozoan group. Also, protozoan grazing rate on phytoplankton removed from 35 to 95% of daily primary production.

9) Mesozooplankton abundance and composition

Copepods constitute >70% of the total mesozooplankton biomass in Arctic waters, where they play a major role in energy flow and biogeochemical cycles. Some of the ingested organic carbon of zooplankton is used for metabolic activities, so quantifying this carbon is of prime importance to better understand energy transfer and elemental cycling via zooplankton in Arctic ecosystems. The Chukchi Sea is one of the major gateways into the Arctic where large quantities of Pacific heat, nutrients, phytoplankton and mesozooplankton enter the region through the shallow Bering Strait in a complicated mixture of water masses. Mesozooplankton abundance and biomass generally have been considered to be low in the Arctic Ocean. Nevertheless, mesozooplankton is numerically important element and plays a major role in the food webs. Mesozooplankton grazing, especially copepods, is a key factor controlling composition and dynamics of phytoplankton communities. In the Arctic Ocean, *Calanus* spp. are regarded as biological indicators of Arctic (*Calanus glacialis* and *C. hyperboreus*) and Atlantic (*C. finmarchicus*) water masses, respectively. They are the most important biomass species and the prime herbivores in these waters. Over the past several decades, atmospheric warming has increased the Arctic Ocean temperature and resulted in decreased extent and thickness of sea ice. The removal of seasonal and permanent sea ice can greatly influence a number of important ecological processes such as photochemical reactions, stratification-related nutrient supply, phytoplankton bloom patterns and mesozooplankton distribution. For predicting climate change impacts in the ecosystems by rapid sea ice melting, it is important to understand the dynamics of the mesozooplankton community. The primary objectives were to understand the interactions between the environmental factors (i.e. seawater temperature, salinity and chlorophyll a concentration) and the mesozooplankton community. In this study area, zooplankton abundance varied from 140 to 3100 indiv. m⁻³, and zooplankton group were dominated by *Eucalanus bungii* and *Calanus glacialis*.

10) Phytoplankton physiology (photochemistry)

Fig. 3.10.1 shows the station map and the average maximal fluorescence (Fm), quantum efficiency of PSII (Fv/Fm) and functional absorption cross section (σ_{PSII}) in the mixed layer. The maximal fluorescence parameter indirectly indicates the biomass of phytoplankton. The values of Fm were higher in the Bering Strait than that in the southern Chukchi Sea. This means that phytoplankton biomass was significantly different in the two regions. The values of Fv/Fm were higher than 0.5 at all stations and there was no regional difference in the Fv/Fm. This indicates that the nutrient limitation for phytoplankton photosynthesis is low in the surface layer. The values of σ_{PSII} represented 400-500 $\text{A}^2 \text{ photon}^{-1}$ at all station but more than 600 $\text{A}^2 \text{ photon}^{-1}$ at station 8 and 9. The large values of σ_{PSII} may be due to the size of phytoplankton community. This will be compared with phytoplankton community data.

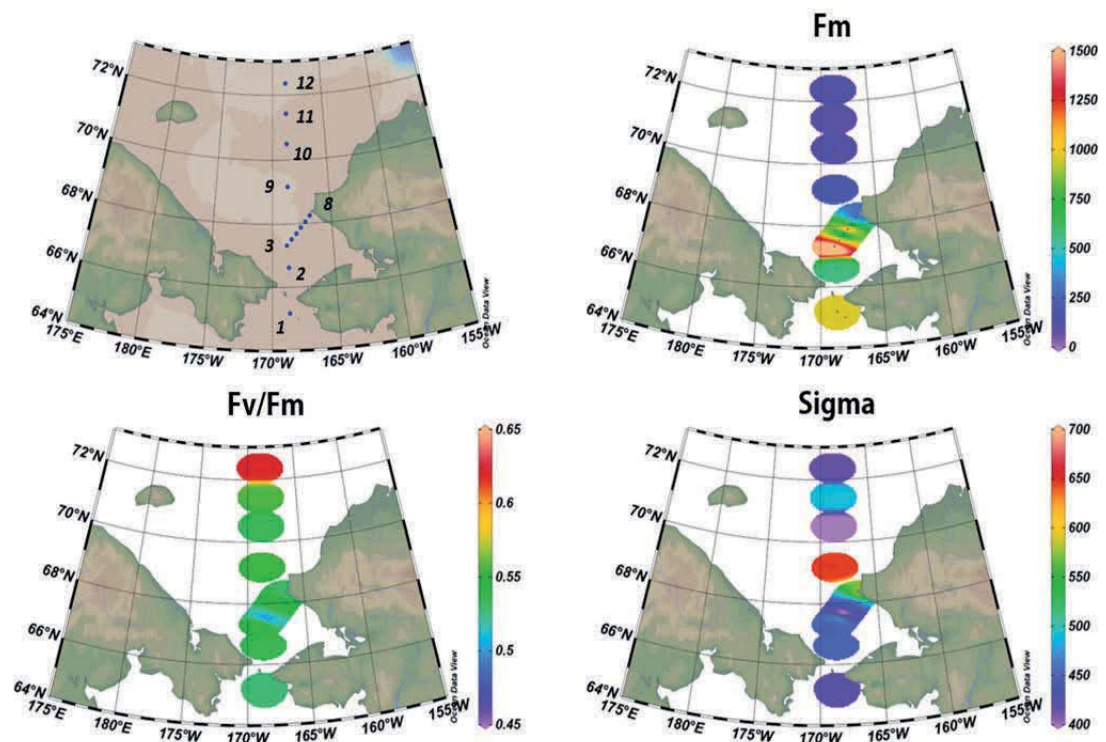


Fig. 3.10.1. Station map and the spatial distributions of maximal fluorescence (Fm), quantum efficiency of PSII (Fv/Fm) and functional absorption cross section (σ_{PSII}).

Vertical distribution of three fluorescence variables is shown in Fig. 3.10.2. The values of F_m were high in the surface layer from station 1 to station 8, and were high at the depth of 30 m from station 9. This represented that the vertical distribution of phytoplankton was different between the Bering Strait and the southern Chukchi Sea. On the other hand, F_v/F_m was similar at all depths. The σ_{PSII} values were relatively high at station 8 and 9. As with the surface layer, it is necessary to compare it with phytoplankton community data at all depths. Overall, phytoplankton biomass and vertical distribution were distinctly different, but F_v/F_m was similar between the Bering Strait and the southern Chukchi Sea. Phytoplankton community data will be compared with the fluorescence variables at each station.

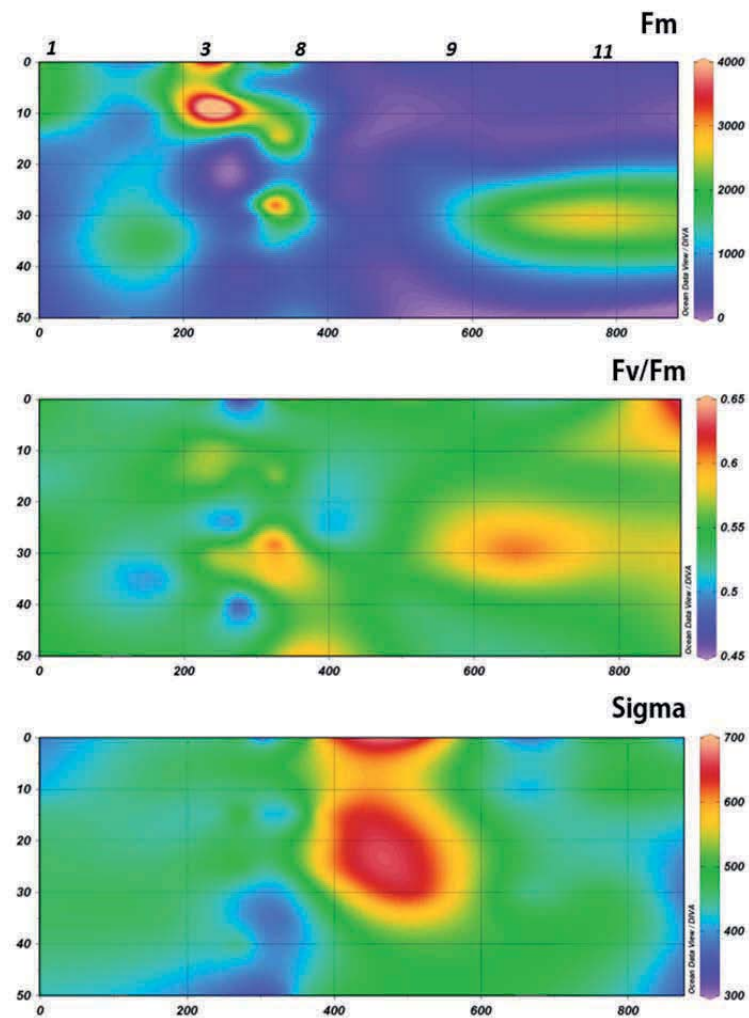


Fig. 3.10.2. Cross-sectional views of maximal fluorescence (F_m), quantum efficiency of PSII (F_v/F_m) and functional absorption cross section (σ_{PSII}).

11) Ocean Optical Observation

The results from the IOPs will be able to show the bio-optical characteristics in water at each station and at each depth of the water sample (Fig. 3.11.1).

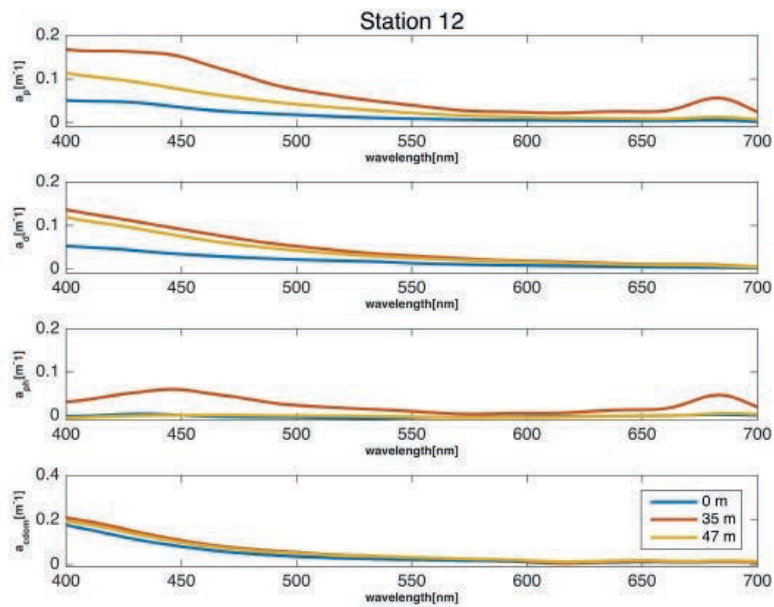


그림 3.11.1. An example of absorption coefficient of particle, de-pigment particle, phytoplankton and colored dissolved organic matter at the station 12.

During this Arctic cruise, data for calibration/validation of satellite remote sensing ocean color data were collected. The IOPs reflected the bio-optical characteristics in water at the selected depths. The results from the AOPs, i.e. data from HPRO II and TriOS, reflect the continuous bio-optical characteristics of water surface and the bio-optical profiles at the operated station (Fig. 3.11.2). We are going to use these field data for further detailed examination and correction of satellite data.

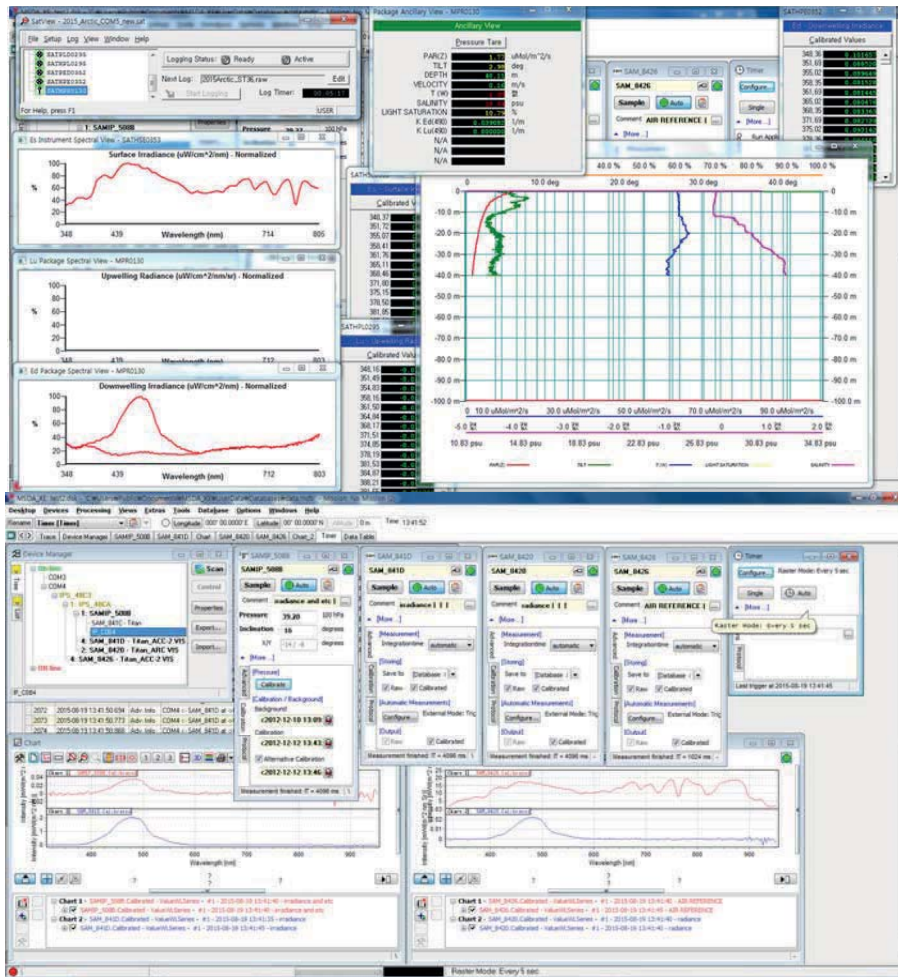


Fig. 3.11.2. An example of HPRO II (up) and TriOS (down) data signal recorded at the station 36.

12) Atmospheric Observations

The statistical distribution of true wind directions and speeds observed during the cruise are shown in Fig. 3.12.1 as a wind rose plot. In 2015, the northwesterlies prevailed and the maximum wind speeds were between 10-15 m/s.

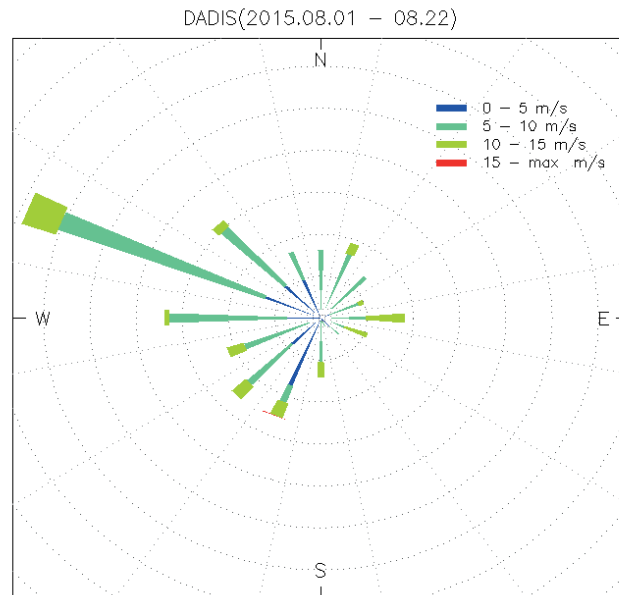


Fig. 3.12.1. Distribution of wind directions and speeds during 2015 Araon Arctic expedition.

Air temperature records measured by HMP45D at the radarmast (38 meters ASL) are shown in Fig. 3.12.2. On the second and third days of cruise (August 2-3, UTC), IBRV Araon entered the Arctic Circle (north of 66°N) and continued cruising to the north. Air temperature dropped quickly below the freezing level while the vessel voyaged northeastward through the Chukchi Sea. Average air temperature in the Arctic was about -1°C and the minimum was about -3.8°C just prior to the sea ice camp.

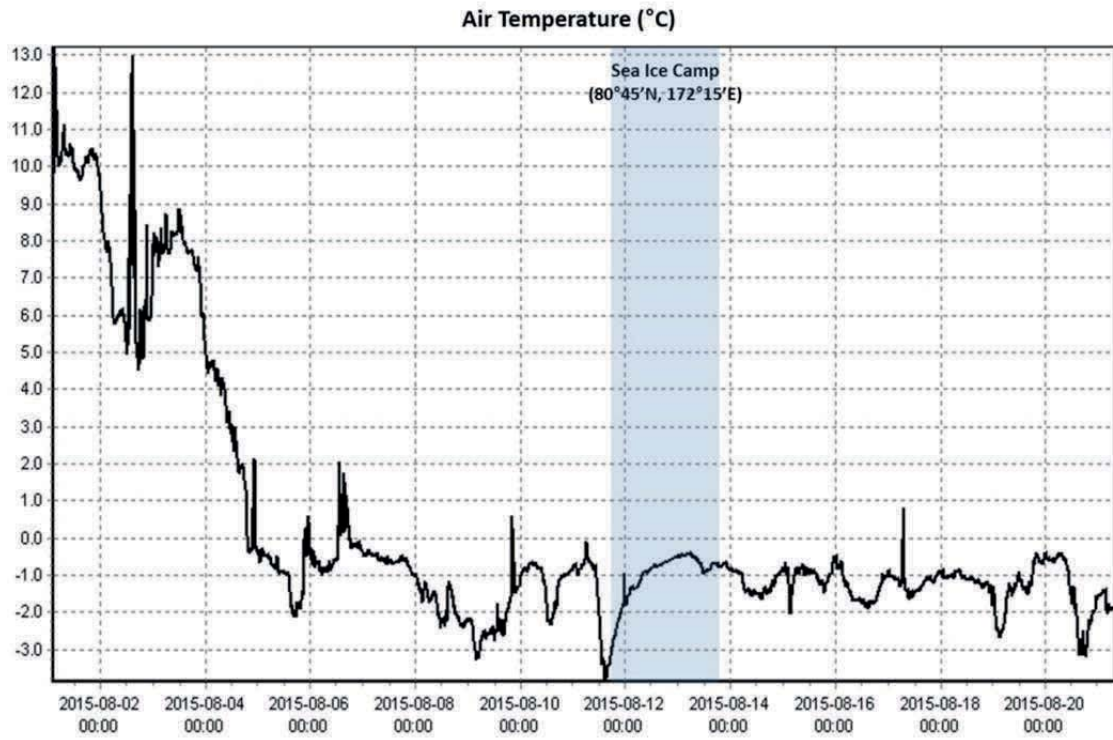


Fig. 3.12.2 Time series of air temperature during 2015 Araon Arctic expedition.

4. Publications

We have not yet published papers in scientific journals out of the results from the expedition. However, several papers have been presented in various meetings held in domestic and foreign countries.